Supporting Information

Takemoto et al. 10.1073/pnas.0812781106

SI Text

Contamination of Cones in the Rod Samples. In Fig. S2*B* a weak signal of anti-GC-C was seen in rod membranes. Our estimated content of GC-C in this rod membrane fraction was 0.15 ± 0.13 (n = 3) per 1,000 rod pigments. This amount of GC-C in the rod membrane fraction was comparable with the expected amount of GC-C that was brought about by contaminated cones: cones contaminated in our purified rod preparations (1.3 ± 1.0% as the pigment ratio; n = 10) would give the signal of 0.32 (24 per 1,000 cone pigments × 0.013) GC-C molecules per 1,000 rod pigments. Similarly, a weak signal of GCAP3 was seen in the rod soluble fraction (Fig. S5B). This signal could also be explained as the contaminated cones that express high content of GCAP3.

Estimation of Concentrations of GCAP-Bound and -Unbound Form of GC. To evaluate the GC activity in intact rods and cones, we estimated the concentration of GCAP-bound and -unbound form of GC in rods and cones. Under equilibrium, the following relation holds in the reaction [**2**]:

$$k_{+1}[\mathrm{GC}]_{\mathrm{free}}\cdot[\mathrm{GCAP}]_{\mathrm{free}} = k_{-1}[\mathrm{GC}\cdot\mathrm{GCAP}], \qquad [4]$$

where $[GC]_{free}$ and $[GCAP]_{free}$ are the concentrations of GC and GCAP that are not bound to GCAP or GC, respectively. As shown in Fig. 2, we estimated the concentration of a GC subtype ($[GC]_{total}$) and that of a GCAP subtype ($[GCAP]_{total}$) in rods and cones. Then, Eq. **4** can be transformed to:

$$([\mathrm{GC}]_{\mathrm{total}} - [\mathrm{GC}\cdot\mathrm{GCAP}])\cdot([\mathrm{GCAP}]_{\mathrm{total}} - [\mathrm{GC}\cdot\mathrm{GCAP}]) = K_{\mathrm{mGCAP}}\cdot[\mathrm{GC}\cdot\mathrm{GCAP}], \qquad [5]$$

where K_{mGCAP} equals k_{-1}/k_{+1}. The K_{mGCAP} value of the binding of each pair of GC and GCAP was determined in the present study (Table 1).

In Eq. **5**, the concentration of GCAP should be that in the OS. Unfortunately, distribution of GCAP1 and GCAP2 in the OS and in other parts of a rod has not been determined in detail (1, 2). To address this point, we tried to quantify GCAPs in the OS and in the IS in rods and cones by using OS-rich and IS-rich samples as we used for determination of GC distribution in rods and cones (Fig. S3). However, we could not obtain reproducible results, and the determination of distribution of GCAP was difficult probably because carp GCAPs became soluble and were lost during detachment of the OS from the IS during preparation of the OS-rich and IS-rich preparations. In previous studies, using serial section with quantitative immunoblot analysis, it was reported that GCAP1 and GCAP2 are expressed mainly in photoreceptor OS (3). In addition, immunocytochemical analysis of human retina showed that GCAP3 is expressed in the COS (4). Based on these findings, we assumed that all of the GCAPs are present in the OS.

By solving Eq. **5** for [GC·GCAP] in the presence of both GCAP1 and GCAP2 for rods, and only GCAP3 for cones, we obtained the concentrations of the GC·GCAP complexes. Because the activity of a single molecule of GC with and without GCAP was determined (Table 1), the activity of GC in rods (summed activities of free GC-R, GCAP1-bound GC-R, and GCAP2-bound GC-R), and that in cones (summed activities of free GC-C and GCAP3-bound GC-C) were calculated (Fig. 5).

Preparation of Rod and Cone Homogenates. Carp (*C. carpio*) rods and cones were isolated and purified with Percoll stepwise density gradient as described (5, 6). The purified rods and cones were washed with a potassium-gluconate buffer (K-gluc buffer: 115 mM potassium gluconate, 2.5 mM KCl, 2 mM $MgCl_2$, 0.2 mM EGTA, 0.1 mM $CaCl_2$, 1 mM DTT, 10 mM Hepes, pH 7.5), and stored at −80 °C until use for 1 week to 6 months. Stored rods or cones were thawed and suspended in the K-gluc buffer and used as a homogenate or centrifuged (100,000 × g, 20 min) to obtain a membrane and a soluble fraction. The period of storage did not affect the GC activity.

Measurement of GC Activity. GC activity was measured based on the method described in ref. 7. The reaction was started by addition of 10 μL of the K-gluc buffer containing (in final concentrations) 1 mM [α-^{32}P] GTP, 2.5 mM [^{3}H] cGMP, 0.1 mM ATP, 0.6 mM 3-isobutyl-1-methyl xanthine (IBMX), 4 mM $MgCl_2$, and 0.3–0.5 mM $CaCl_2$ or 0.8 mM EGTA to 15 μL of rod or cone homogenates containing (in final concentrations) 6 μM rod pigment or 0.5 μM cone pigment. When GCAP was added, it was mixed with rod or cone homogenates before the assay. The assay was performed at 25 °C and terminated by addition of 40 μL of 0.4 M HCl. A portion of the sample (40 μL) was added to 150 mg of Alumina N, Akt. I (ICN) and suspended in 500 μL of a Tris buffer (50 mM EDTA, 200 mM Tris·HCl, pH 7.4). Then the sample was mixed well and centrifuged for 15 min at 20,000 × g. A portion (40 μL) of the supernatant was mixed with 4 mL of a liquid scintillation mixture (Clear-sol I; Nakalai Tesque), and both ^{3}H and ^{32}P radioactivity were counted with a liquid scintillation counter (LS 6500; Beckman). Although the pigment concentration was 12 times higher in the measurement in rod samples than in cone samples, the pigment concentration did not affect the measured GC activity significantly within the range of the pigment concentrations we examined: 1–6 μM in rod membranes and 0.5–3 μM in cone membranes.

Determination of Content of Visual Pigment. GC activity is expressed in the unit of cGMP synthesized per visual pigment. The amount of visual pigment was determined spectrophotometrically (5). In rods, the pigment concentration was determined by the difference of the absorbance at 520 nm before and after bleach with >440 nm light (VY46 filter; Toshiba) by using a tungsten lamp (100 W) in the presence of 10 mM NH_2OH with the molar absorption coefficient of 40,000. Cone membranes were mixed with a buffer containing 0.75% CHAPS, 1 mg/mL phosphatydylcholine, 50 mM Hepes, 140 mM NaCl, 2 mM $MgCl_2$, 20% (wt/vol) glycerol, 1 mM DTT (pH 7.5) and were continuously stirred overnight at 4 °C in the dark. The mixture was centrifuged (100,000 × g, 15 min) to obtain CHAPS-solubilized cone pigments. To quantify the amount of each pigment type, a partial bleaching method was applied in the presence of 10 mM NH_2OH. The sample was first irradiated with >660 nm light (VR68 filter; Toshiba) more than 10 min until the absorption spectrum did not change further with additional irradiation of the same light. The difference of the absorbance at 618 nm before and after the irradiation was taken as a measure of the content of red pigment. Then irradiation was repeated successively but with light containing different wavelengths. The content of green pigment was then determined at 535 nm by irradiating the sample with >600 nm light (VR62 filter; Toshiba), and the content of blue pigment was determined at 460 nm by giving >520 nm light (VO54; Toshiba). The content of UV pigment was difficult to determine spectrophotometrically, but its amount was the lowest compared with those of other cone

pigment types. The amount of each bleached pigment was quantified by assuming that their molar absorption coefficients were similar to that of rhodopsin, i.e., 40,000. The relative amount of the cone pigment types in our preparation was ≈3:1:1 (red/green/blue) (5).

Isolation of cDNA Clones for GCs and GCAPs. To determine the carp GC-R1, GC-R2, and GC-C sequences, we synthesized degenerated primers based on the amino acid sequence conserved among these teleost proteins (Table S1). For the determination of the sequence of GC-R1, both 5′ and 3′ RACE were performed by using a carp retinal cDNA library as the template. Subsequently, RT-PCR was performed by using gene-specific primers for the 5′ and 3′ edges of the GC-R1 coding region. For determination of GC-R2 and GC-C sequences, we amplified target fragments from a carp retinal cDNA by RT-PCR. Using these partial sequences as probes, the carp retinal cDNA library was screened, and the full length of the cDNAs corresponding to GC-R2 and GC-C was obtained.

To obtain cDNA clones of carp GCAPs, we synthesized oligonucleotides corresponding to the amino acid sequences conserved among the teleost proteins. Using these oligonucleotides (Table S1) as primers, cDNA fragments of each GCAP were amplified from a carp retinal cDNA by RT-PCR. A partial sequence of carp GCAP2 had been obtained (8). Partial sequences of GCAP1, GCAP2, and GCAP3 thus obtained were used to screen the carp retinal cDNA library to determine the full length of the corresponding cDNAs. We performed RT-nested PCR to obtain DNA fragments corresponding to GCAP4, GCAP5, and GCAP7. To obtain the coding region sequences of GCAP4, GCAP5, and GCAP7, we performed 5′ and 3′ RACE. The nucleotide sequences were determined with an ABI PRISM 3100 DNA sequencer (Applied Biosystems).

Expression and Purification of GCAPs. Each GCAP gene was subcloned into a pET3 or pET16 vector (Novagen). The restriction site of appropriate restriction endonuclease was attached to the 5′ or the 3′ end of the coding region of a GCAP gene by PCR, and the resultant product was ligated into pET3a or pET16b (Table S3). These constructs, including that of medaka GCAP, were used to express N-myristoylated GCAPs in *E. coli*.

Expression of GCAP in *E. coli* was carried out as described (7). Carp GCAP1 was not stably expressed. So, instead of carp GCAP1, medaka GCAP1 was expressed in *E. coli.* Most GCAPs were expressed at 37 °C, but induction of GCAP5 was performed at 16 °C for 25–30 h. After expression of GCAPs in *E. coli*, cells were resuspended in a Tris-EGTA buffer (50 mM Tris·HCl, 1 mM EGTA, pH 7.5) and sonicated. Most GCAPs except GCAP5 were found in insoluble inclusion bodies that were subsequently solubilized and dialyzed. The soluble fractions containing these GCAPs were obtained by centrifugation (27,000 × *g* for 15 min at 4 °C). GCAP5 was obtained in the soluble fraction, which was directly used for purification. Carp GCAP1 was expressed in Sf9 cells by using Bac-to-Bac Baculovirus Expression Systems (Invitrogen). Cells were collected by centrifugation (3,500 × *g* for 15 min at 4 °C), freeze-thawed, sonicated, and centrifuged (27,000 × *g* for 15 min at 4 °C) to obtain a soluble fraction containing GCAP1.

The fractions containing GCAPs were first loaded to a DEAE-Sepharose CL6B column (GE Healthcare Biosciences) and washed with the Tris-EGTA buffer containing 100–180 mM NaCl. GCAPs were eluted with the Tris-EGTA buffer containing 280–350 mM NaCl. Then, $CaCl_2$ and $MgCl_2$ were added to the sample at their final concentrations of 2 mM, and the sample was applied to a Phenyl-Sepharose CL4B column (GE Healthcare Biosciences). After the sample was washed with a buffer (50 mM Tris·HCl, 2 mM $MgCl_2$, 1 mM $CaCl_2$, 1 mM DTT, pH 7.5), most of the GCAPs were eluted with an elution buffer 1 (20 mM Tris·HCl, 2 mM $MgCl_2$, 3 mM EGTA, 1 mM DTT, pH 8.5). For medaka GCAP1, elution buffer 2 (10 mM Tris·HCl, 2 mM $MgCl_2$, 3 mM EGTA, 1 mM DTT, pH 8.5) was used, and for carp GCAP1, elution buffer 3 (5 mM Tris·HCl, 2 mM $MgCl_2$, 3 mM EGTA, 1 mM DTT, pH 8.5) was used. Fractions containing GCAPs were concentrated and buffer-exchanged into the K-gluc buffer by using Vivaspin (Sartorius). The purity of GCAPs used was 65–82%. By a protein sequencer analysis, the N termini of the expressed GCAP1 and GCAP3 were confirmed to be blocked, most probably with myristic acid as is in the case of native GCAPs. On the other hand, a large portion (78%) of GCAP2 was not blocked, which indicated that the N terminus of this portion was not myristoylated. In the estimation of the in situ GC activity in rods (Fig. 5), therefore, we assumed that the myristoylation of GCAP2 increases the GC activity by 1.5-fold (9).

Quantification of GCs and GCAPs in Rods and Cones by Immunoblot. Coding regions of the C-terminal sequences of GC-R1 and GC-R2 genes corresponding to amino acid residues 1076–1107 and 1022–1076, respectively, were inserted into the EcoRI/XhoI sites in pGEX 5X-1 vector (Invitrogen) and expressed in *E. coli* BL21 cells as fusion peptides of GST linked at the N terminus of each peptide. The peptides were purified according to the manufacturer's instructions. Mice were immunized with these peptides to obtain anti-GC-R1 and anti-GC-R2 antiserum. A rabbit was immunized with a C-terminal peptide (residues 1123–1141) of GC-C anchored to keyhole limpet hemocyanin at the N terminus of the peptide to obtain anti-GC-C antiserum. Anti-GC-C specific antibody was obtained by further affinity purification with the GC-C peptide. Anti-GCAP1, GCAP2, GCAP3, and GCAP5 antiserum were raised against recombinant medaka GCAP1, carp GCAP2, carp GCAP3, and carp GCAP5 in mice, respectively.

To quantify the expression levels of GCs, C-terminal partial peptides of GC fused to MBP at the peptide N-terminal were used as the standards for immunoblot analysis (10). C-terminal sequences of GC-R1, GC-R2, and GC-C genes corresponding to amino acid residues 1026–1107, 1022–1076 and 1059–1141, respectively, were inserted into the EcoRI/XhoI sites in pMAL c2E vector (New England BioLabs), expressed in *E. coli* BL21 cells, and purified according to the manufacturer's instructions. The estimated results of the GC content with use of MBP-fusion peptides as the molar standard were compared with those determined in different methods. In rods, by quantification with CBB staining, an immunopositive ≈120-kDa protein band containing GC-R1, the major GC in rods, was quantified. In cones, because of limitation of the sample, we tried to quantify GC-C in cones by immunoblot with use of GC-C that was expressed in COS cells and was quantified with CBB staining at an immunopositive ≈120-kDa protein band. Because the protein band containing GC-R1 may contain other proteins and the expression level of GC-C in COS cells was very low, the contents of GCs estimated in these methods may be rough indicatives of the contents of GC-R1 and GC-C. However, the contents of GCs determined in these methods were similar to those determined with use of MBP fusion peptides: 1.3 (with an MBP fusion peptide) and 2.5 (with CBB staining) GC-R1 per 1,000 rhodopsin molecules, and 24 (with an MBP fusion peptide) and ≈10 (with GC-C expressed in COS cells as the standard) per 1,000 cone visual pigments. To quantify GCAPs, recombinant GCAPs were used.

Expression levels of GCs and GCAPs were determined by immunoblot as described (6). In the course of this study, we realized that some of the GCs passed through the blotted membrane. To avoid the loss of GCs, by using 2-ply membranes, we searched for the conditions in which GCs under study were retained on the blotting membrane. Based on the results of these

control studies, we used 7.5% polyacrylamide gel, and depending on the GC subtype, we used different concentrations of SDS for the electroblotting: 0.05% SDS for GC-R1, GC-C, and MBP-fused C-terminal peptides of GC-R1 and GC-C; 0.025% SDS for GC-R2; and 0.1% SDS for the MBP-fused C-terminal peptide of GC-R2. We confirmed that proteins were not left in the gel. For quantification of GCAPs, to avoid the appearance of the doublet bands of GCAP (Ca^{2+}-free and Ca^{2+}-bound forms), 1 mM $CaCl_2$ was added in the 12.5% polyacrylamide gel.

GCs, GC fusion peptides, and native/recombinant GCAPs were probed immunologically and detected by Chemi-Lumi One L (Nacalai Tesque) using HRP-labeled anti-mouse or anti-rabbit IgG antibodies as secondary antibodies. The content of a protein was expressed as the ratio to that of visual pigment.

Measurements of Membrane Currents from tROS and tCOS Preparations. The membrane current of a frog tROS or a carp red tCOS was measured after perfusion with exogenous 1 mM cGMP or 1 mM GTP as described (11). Bullfrogs (*Rana catesbeiana*) or carp were dark-adapted and their retinas were dissected. Photoreceptors were mechanically dissociated in Ringer's solution. The OS was sucked into an electrode filled with a choline solution (115 mM choline chloride, 2.5 mM KCl, 2 mM $MgCl_2$, 0.2 mM EGTA, 0.1 mM $CaCl_2$, 10 mM Hepes, pH 7.5) and the exposed part outside of the electrode (IS plus basal part of the OS) was truncated with a fine glass rod under visual control with the aid of an IR television monitor. In the case of frog tROS, the length of the sucked ROS had a significant effect on the time course of the current rise induced by cGMP: when the tROS length was 12–14 μm, the current saturated within a few seconds as shown in Fig. 4*B* (thin black traces), whereas at 36–45 μm it took >10 s to saturate. It was probably because it took time for cGMP to diffuse widely in the tROS. For this reason, the length of tROS was made as short as possible (12–14 μm). The inside of the OS was perfused with the K-gluc buffer containing 0.5 mM IBMX, 0.2 mM ATP, and either 1 mM cGMP or 1 mM GTP. After truncation, first 1 mM cGMP was perfused to monitor the diffusion of a small molecule like cGMP. Then the inside of the OS was washed with the K-gluc buffer containing 0.2 mM ATP, and after the membrane current diminished, 1 mM GTP was perfused. Membrane current was monitored with a patch-clamp amplifier, EPC-7 (List).

1. Dizhoor AM, et al. (1995) Cloning, sequencing, and expression of a 24-kDa Ca^{2+}-binding protein activating photoreceptor guanylyl cyclase. *J Biol Chem* 270:25200–25206.
2. Kachi S, et al. (1999) Detailed localization of photoreceptor guanylate cyclase activating protein-1 and -2 in mammalian retinas using light and electron microscopy. *Exp Eye Res* 68:465–473.
3. Strissel KJ, et al. (2005) Recoverin undergoes light-dependent intracellular translocation in rod photoreceptors. *J Biol Chem* 280:29250–29255.
4. Imanishi Y, et al. (2002) Characterization of retinal guanylate cyclase-activating protein 3 (GCAP3) from zebrafish to man. *Eur J Neurosci* 15:63–78.
5. Tachibanaki S, Tsushima S, Kawamura S (2001) Low amplification and fast visual pigment phosphorylation as mechanisms characterizing cone photoresponses. *Proc Natl Acad Sci USA* 98:14044–14049.
6. Tachibanaki S, et al. (2005) Highly effective phosphorylation by G protein-coupled receptor kinase 7 of light-activated visual pigment in cones. *Proc Natl Acad Sci USA* 102:9329–9334.
7. Hurley JB, Dizhoor AM (2000) Heterologous expression and assays for photoreceptor guanylyl cyclases and guanylyl cyclase-activating proteins. *Methods Enzymol* 315:708–717.
8. Shimauchi-Matsukawa Y, Aman Y, Tachibanaki S, Kawamura S (2008) Identification of differentially expressed genes in carp rods and cones. *Mol Vis* 14:358–369.
9. Hwang JY, Koch KW (2002) Calcium- and myristoyl-dependent properties of guanylate cyclase-activating protein-1 and protein-2. *Biochemistry* 41:13021–13028.
10. Helten A, Säftel W, Koch KW (2007) Expression level and activity profile of membrane-bound guanylate cyclase type 2 in rod outer segments. *J Neurochem* 103:1439–1446.
11. Kawamura S, Murakami M (1991) Calcium-dependent regulation of cyclic GMP phosphodiesterase by a protein from frog retinal rods. *Nature* 349:420–423.

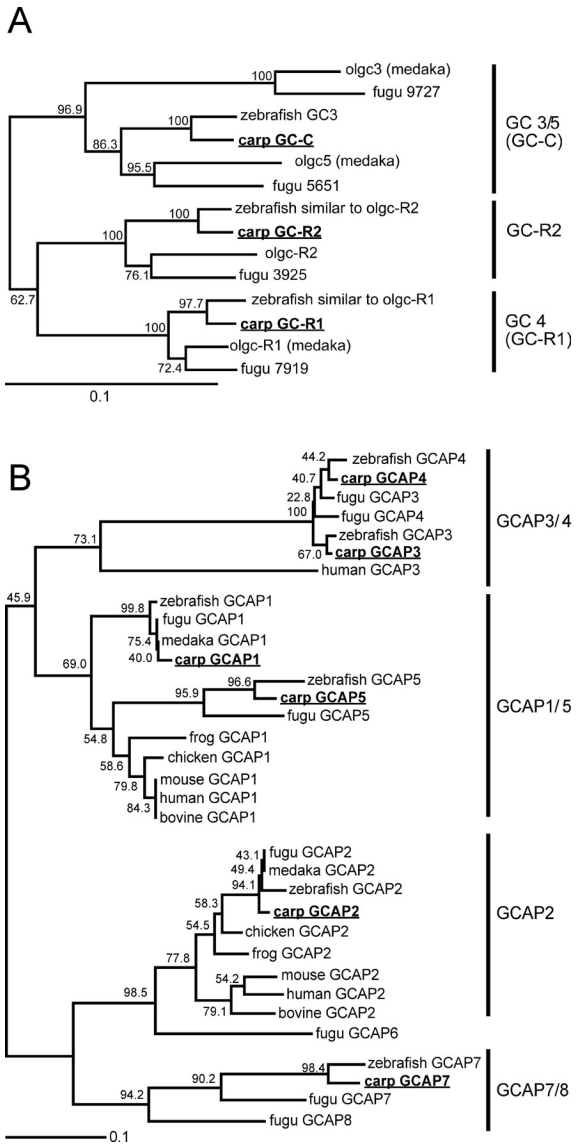

Fig. S1. Phylogenetic relations of cloned carp GCs and GCAPs. A phylogenetic tree constructed from the amino acid sequences of GCs and GCAPs. Amino acid sequences of intracellular regions of GCs (*A*) and the entire sequences of GCAPs (*B*) were aligned with Clustal W. A total of 72 (GCAPs) and 336 (GCs) confidently aligned residues were used for estimating relationships among the proteins analyzed by neighbor-joining using the PHYLIP version 3.5c software package. Confidence in the phylogeny was assessed by bootstrap resampling of the data. Numbers at the nodes indicate the clustering percentage obtained from 1,000 bootstrap resamplings. Bar indicates 10% replacement of an amino acid per site.

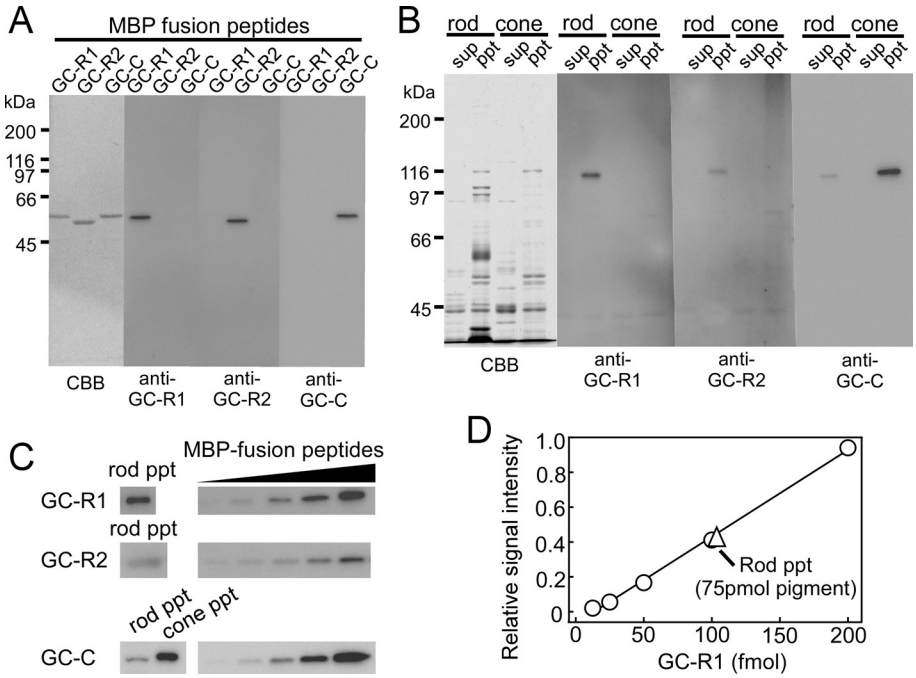

Fig. S2. Quantification of GCs in rods and cones. (*A*) Specificity of antiserum or antibody used. MBP-fused C-terminal partial peptides of GC-R1, GC-R2, and GC-C (100 fmol of each) were probed by immunoblot with anti-GC-R1 antiserum, anti-GC-R2 antiserum, and affinity-purified anti-GC-C antibody. The CBB-stained bands of 2 pmol of the MBP-fused peptides are shown at left. (*B*) Distribution of GCs in rods and cones. Soluble (sup) and membrane (ppt) fractions were obtained from purified rod (containing 50 pmol pigment) and cone (containing 2.5 pmol pigment) homogenates. Each fraction was probed by immunoblot with anti-GC-R1 antiserum, anti-GC-R2 antiserum, and anti-GC-C antibody. The CBB-stained bands of rod and cone proteins are shown at left . (*C*) Quantification of GCs in rods and cones. Immunoblot signals of anti-GC-R1 antiserum (*Top*), anti-GC-R2 antiserum (*Middle*), and anti-GC-C antibody (*Bottom*) were obtained in the membrane fractions of rods (rod ppt) and cones (cone ppt). Known molar amounts of MBP fusion peptides of the C-terminal regions of GC-R1, GC-R2, and GC-C were also blotted and visualized simultaneously with GC signals. (*D*) An example of quantification of GC-R1 by immunoblot. In the calibration curve obtained by immunoblot of known molar amounts of an MBP fusion peptide of GC-R1 (○), the signal from a rod membrane fraction containing 75 pmol of rod pigment was plotted (△).

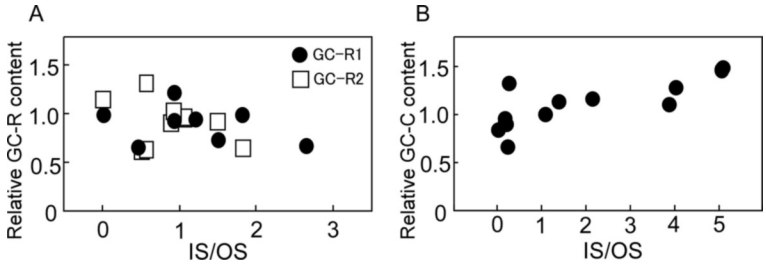

Fig. S3. Distribution of GCs in rods and cones. (*A*) GC-R1 and GC-R2 were quantified with immunoblots in rod preparations having different content of RIS relative to that of ROS. The content of GC-R1 or GC-R2 in each preparation was plotted against the IS/OS ratio. The IS/OS ratio in the starting rod sample used for preparation of the IS-rich and the OS-rich sample was taken to be 1.0. The measured GC-R1 and GC-R2 contents were normalized to the amounts of GC-R1 and GC-R2, respectively, contained in the starting rod sample. (*B*) Similar to *A*, but GC-C was quantified in cone preparations having different contents of CIS.

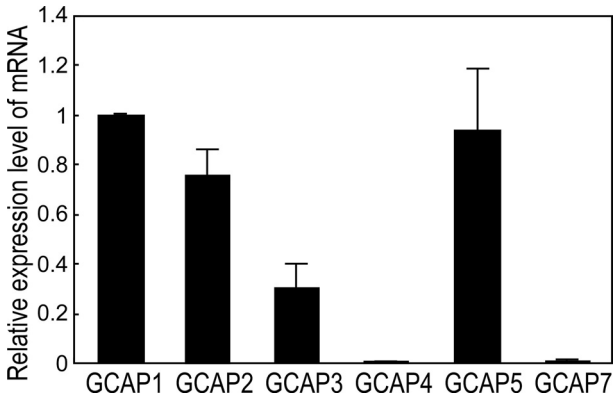

Fig. S4. Expression levels of GCAP mRNAs in the carp retina. Relative abundance of 6 GCAP mRNAs was measured in the carp retinal cDNA with real-time RT-PCR. The level of each mRNA was normalized to that of GCAP1. The result is shown as mean ± SD ($n = 3$).

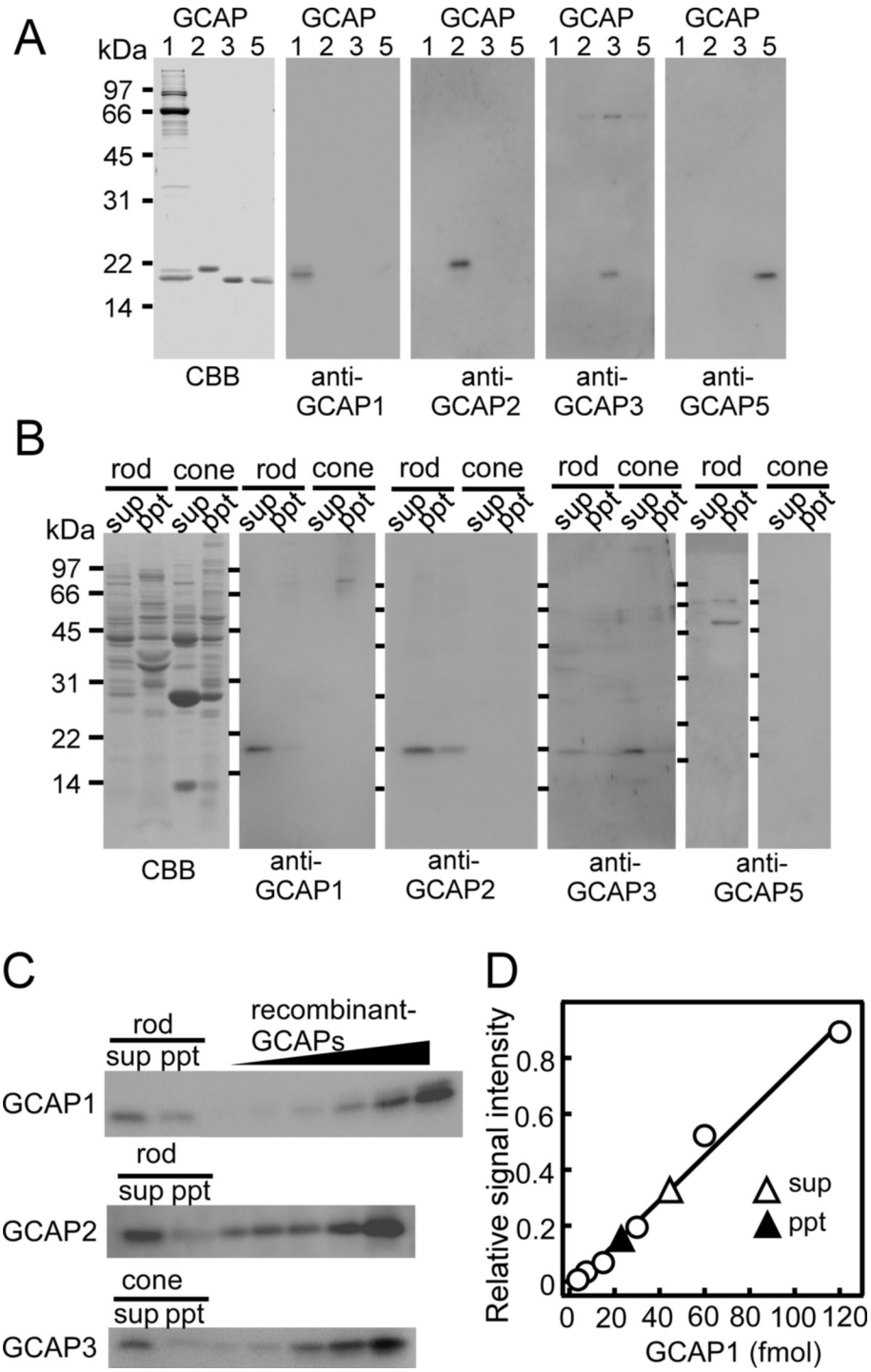

Fig. S5. Quantification of GCAPs in rods and cones. (*A*) Specificity of anti-GCAP antiserum used. Recombinant proteins of GCAP1, GCAP2, GCAP3, and GCAP5 (100 fmol each) were probed by each of anti-GCAP1, anti-GCAP2, anti-GCAP3, and anti-GCAP5 antiserum. The CBB-stained bands of 10 pmol of each recombinant protein are shown at left. (*B*) Distribution of GCAPs in rods and cones. Soluble (sup) and membrane (ppt) fractions obtained from purified rod (containing 250 pmol pigment) and cone (containing 5 pmol pigment) homogenates were probed by specific antiserum against GCAP1, GCAP2, GCAP3, and GCAP5. (*C*) Quantification of GCAPs in rods and cones. Immunoblot signals were obtained in the soluble (sup) and the membrane (ppt) fractions of rods and cones, and known amounts of recombinant GCAPs. (*D*) An example of quantification of GCAP1 by immunoblot. In the calibration curve obtained by immunoblot of known amounts of standard recombinant GCAP1 (○), the signals from a soluble (△) and a membrane (▲) fraction prepared from a rod sample containing 75 pmol of rod pigment were plotted.

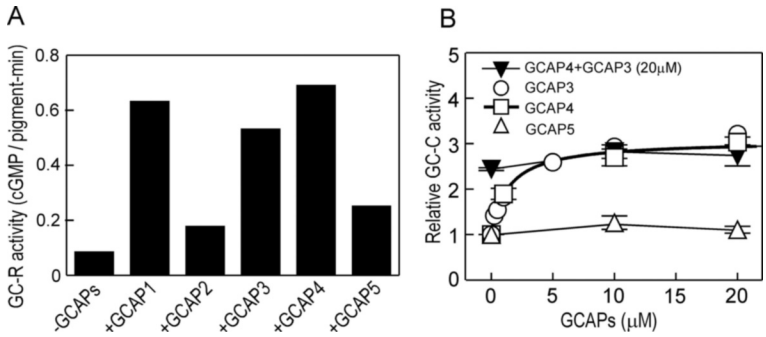

Fig. S6. Regulation of GC activities by GCAP subtypes. (*A*) GC activities in the presence of various subtypes of GCAP (10 μM each) in rod homogenates. Measurements were made at a low Ca^{2+} concentration. (*B*) Dose-dependent activation of GC by GCAP3, GCAP4, and GCAP5 in cone homogenates. Relative GC activity, normalized to the GC activity without recombinant GCAPs, was plotted against the final concentration of added proteins. Recombinant carp CGAP1–3 and zebrafish GCAP4 (NM_001011661) and GCAP5 (NM_200656) were used.

Table S1. Primers used in RT-PCR

GC type	Nested PCR	Sense primer	Antisense primer
GC-R1	1st PCR	5′-TYMTYYTBGGHGTGYTGA-3′	5′-GCGATTTCAGCTGCATGCTT-3′
	2nd PCR	5′-ACRTTYCCWYGYTGYGTCC-3′	5′-AGACATCGTGGTTGCCCAGC-3′
GC-R2		5′-TTYGCNATHATHATGCARGARGT-3′	5′-GGCATRTGNCKCATYTTRAANGT-3′
GC-C		5′-GTNGARMGNCARAARACNGAYAA-3′	5′-CYTTRAANGTNCCDATRCARTG-5′
GCAP1		5′-TGGTAYAARAARTTYATGACNGA-3′	5′-CCRTCNCCRTTNAYRTCDAT-3′
GCAP3		5′-TGGTAYAAYAARTTYATGMGNGA-3′	5′-TTNCCRTTNCCRTCYTGRTCRAA-3′
GCAP4	1st PCR	5′-GGAAACAGCTATGACCATGATTACGCCAAGCTCGA-3′*	5′-CCYTCNACDATDATNA-3′
	2nd PCR	5′-TGGTAYAAYAARTTYATGMGNGA-3′	5′-GGRTGNTCYTTNGCNCCYTC-3′
GCAP5	1st PCR	5′-CARTGGTAYMGNAARTTYATGAC-3′	5′-TAATACGACTCACTATAGGG-3′*
	2nd PCR	5′-ARTTYTTYGGNYTNAARAA-3′	5′-CCRTCNCCRTTNAYRTCDAT-3′
GCAP7	1st PCR	5′-GGAAACAGCTATGACCATGATTACGCCAAGCTCGA-3′*	5′-CRTCYTTYTSNGCNCC-3′
	2nd PCR	5′-AATTAACCCTCACTAAAGGG-3′*	5′-ATYTGNCCRTCRTTRTTNT-3′

*These primers correspond to sequences contained in pBluescript vector.

Table S2. Primers used in real-time RT-PCR

GCAP type	Sense primer	Antisense primer
GCAP1	5′-TGTGGCTGCTCTCAGTCTTGTAA-3′	5′-GCAGCCGTTGCCATCAA-3′
GCAP2	5′-AGTGAGGATTCGGAAGATAAAGAGATT-3′	5′-CCCGCTCGGACATTCAAC-3′
GCAP3	5′-ATCCAGGACATTACCCGGAGTTA-3′	5′-TTCATTATTGACATCGATCCTCTCATAG-3′
GCAP4	5′-AATATTTACCGCTATACAAGACATCACAA-3′	5′-CCCTCAACATCAATCTTTTCAAATATG-3′
GCAP5	5′-CCATTGAAGCCATTAACGGAGTA-3′	5′-CCATCTCCATTAACATCAATCTTGTT-3′
GCAP7	5′-TTGGACAGACAAGAAGTCAAACG-3′	5′-CGCTGGGTGTCATGTGGAT-3′

Table S3. Primers and vectors used for expression of GCAPs

GCAP type	Vector and restriction site	Sense primer	Antisense primer
Carp GCAP1	pET16b NcoI–BamHI/BglII	5′-CATGCCATGGGGAATTCAACGGGCT-3′	5′-GAAGATCTTTAGACGCTGTGTCTCCGGTT-3′
Carp GCAP2	pET3a NdeI–BamHI	5′-GGAATTCCATATGGGTCAGCGACTCAGTG-3′	5′-CGCGGATCCTCAGAAGTTGGCGCTGCGGCGCGT-3′
Carp GCAP3	pET16b NcoI–XhoI	5′-CATGCCATGGGTGCCCACGGGTCCAGC-3′	5′-CCGCTCGAGTCACTCCTTCTTTTTCTGTCC-3′
Zebrafish GCAP4	pET16b NcoI–XhoI	5′-CCATGGGTAACAACCATGCC-3′	5′-CTCGAGTTATTTCTGTCGCCCTTC −3′
Carp GCAP5	pET16b NcoI–XhoI	5′-CCATGGGAAACACCTCCGGCA-3′	5′-CTCGAGTCAGGCTGGTCTGGGGTCA-3′
Zebrafish GCAP5	pET16b NcoI–XhoI	5′-CCATGGGGGACTCCTCCAGC-3′	5′-CTCGAGTCATGCTTGATCCTCGAT −3′